Fusion Engineering and Design 146 (2019) 1824–1828

Contents lists available at ScienceDirect

Fusion Engineering and Design

journal homepage: www.elsevier.com/locate/fusengdes

Sintering and irradiation of copper-based high entropy alloys for nuclear fusion

M. Dias[a,*], F. Antão[a], N. Catarino[a], A. Galatanu[b], M. Galatanu[b], P. Ferreira[c], J.B. Correia[d], R.C da Silva[a], A.P. Gonçalves[e], E. Alves[a]

[a] Instituto de Plasmas e Fusão Nuclear, Instituto Superior Técnico, Universidade de Lisboa, Av. Rovisco Pais, 1049-001, Lisboa, Portugal
[b] National Institute of Materials Physics, Magurele 077125, Romania
[c] Department of Materials and Ceramics Engineering, CICECO, Universidade de Aveiro, 3810-193 Aveiro, Portugal
[d] LNEG, Laboratório Nacional de Energia e Geologia, Estrada do Paço do Lumiar, 1649-038 Lisboa, Portugal
[e] C²TN, DECN, Instituto Superior Técnico, Universidade de Lisboa, Estrada Nacional 10, 2695-066 Bobadela LRS, Portugal

ARTICLE INFO

Keywords:
High entropy alloys
Microstructure
Irradiation damage
X-ray diffraction

ABSTRACT

In this study, $Cu_xCrFeTiV$ (x = 0.21, 0.44, 1 and 1.7 M ratio) high entropy alloys have been devised for thermal barriers between the plasma facing tungsten tiles and the copper-based heat sink in the first wall of nuclear fusion reactors. The high entropy alloys were produced by ball milling the elemental powders, followed by consolidation with spark plasma sintering. Irradiation of the equiatomic CuCrFeTiV sample was carried out at room temperature with Ar^+ (300 keV) beams with a fluence of 3×10^{20} at/m^2. Structural changes prior and after irradiation were investigated by scanning electron microscopy, coupled with energy dispersive X-ray spectroscopy, X-ray diffraction and thermal diffusivity. Preliminary results showed the presence of heterogenous and multiphasic microstructures in all samples. Moreover, with the increase of the Cu content it is possible to observe the formation of Cu-rich structures. The diffractogram of the CuCrFeTiV sample revealed major peaks of a BCC crystal structure and minor peaks of a FCC crystal structure. In addition, after irradiation no modifications in the CuCrFeTiV microstructure or in the diffractogram were observed.

1. Introduction

The possibility to obtain energy from nuclear fusion is a promising way to fulfill the current and future energy needs of humanity in a clean way. However, a collection of challenges in materials science and engineering must be overcome to be able to achieve conditions for sustained plasma fusion reaction. One of the issues in the divertor, a region of high heat flux, is the fact that its materials must endure high temperatures and irradiation damage, while efficiently extracting the heat for electric power generation. Tungsten, with a high melting point, high sputtering threshold and low tritium inventory [1,2] is the main candidate for plasma facing in this region, and CuCrZr alloy, with high conductivity and strength [3], for heat sinking. The issue arises in a dissimilarity between both materials: the high ductile-brittle transition (DBTT) temperature of tungsten [4] demands higher temperature, while CuCrZr imposes a low service temperature [5] and suffers from radiation embrittlement [6]. This will lead to a less efficient heat extraction and shorter service life-times of the materials in use; therefore, a thermal barrier interlayer is necessary.

High Entropy Alloys (HEAs) are alloys composed of five or more metallic elements, with concentrations between 5 at.% and 35 at.% [7], that can form random simple solid solutions with distorted lattices (mainly BCC or FCC) confering them enhanced properties, instead of the complex and brittle intermetallics that are formed in conventional, non HEA, alloys. Interesting properties were obtained with HEAs that reveal their potential as thermal barriers: high hardness [8], enhanced wear [9], oxidation [10] and corrosion [11,12] resistances, high thermal stability [13], both under continuous and cyclic operation, and intrinsically low thermal conductivity [13,14]. Moreover, recent studies shown that the accumulated lattice strain might confer higher radiation resistance in HEAs [15]. However, the high energy neutrons from fusion reactions are expected to induce atomic displacement cascades in the first wall materials, but the response of the proposed thermal barrier interlayer to irradiation damage is not known and requires elucidation.

In this study the $Cu_xCrFeTiV$ (x = 0.21, 0.44, 1 and 1.7 M ratio) were prepared using mechanical alloying (MA), to mix the elemental powders, followed by consolidation with spark plasma sintering (SPS) at 1178 K and 65 MPa. The equiatomic CuCrFeTiV sintered sample was

* Corresponding author.
E-mail address: marta.dias@itn.pt (M. Dias).

https://doi.org/10.1016/j.fusengdes.2019.03.044
Received 8 October 2018; Received in revised form 6 March 2019; Accepted 7 March 2019
Available online 16 March 2019
0920-3796/

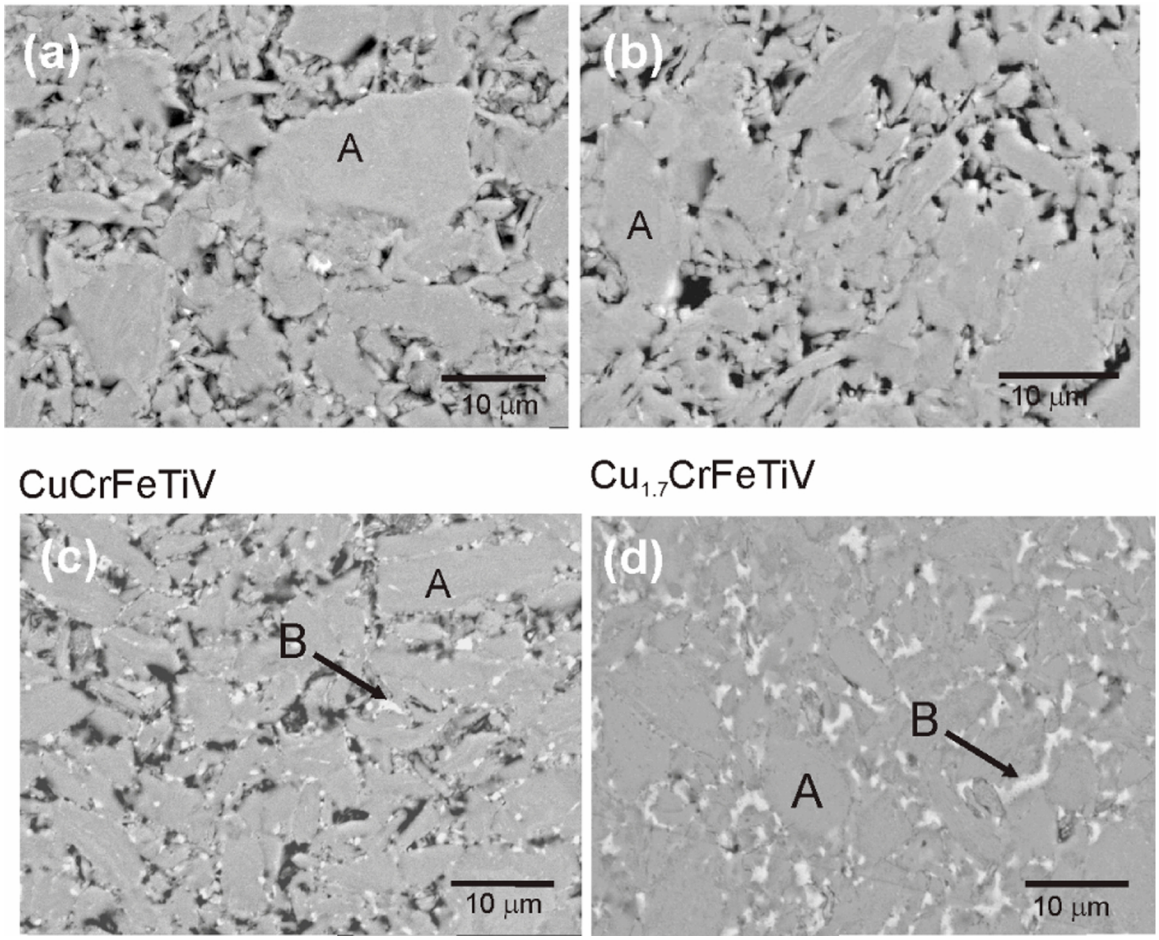

Fig. 1. BSE SEM images of as-sintered (a) $Cu_{0.21}CrFeTiV$, (b) $Cu_{0.44}CrFeTiV$, (c) CuCrFeTiV and (d) $Cu_{1.7}CrFeTiV$ samples.

irradiated at room temperature with 300 keV Ar^+ beam (to a fluence of 3×10^{20} at/m^2) in order to simulate the irradiation damage in the material. Scanning electron microscopy (SEM) coupled with energy dispersive X-ray spectroscopy (EDS), and X-ray diffraction (XRD) were used to characterize the alloys prior to and after irradiation.

2. Experimental details

2.1. Alloys preparation and consolidation

Powders of Cr, Cu, Fe, Ti and V with purity greater than 99.5% and 45 μm particle size (Alpha Aesar) were mixed inside a glove box, with argon atmosphere to prevent oxidation, to obtain the $Cu_xCrFeTiV$ (x = 0.21, 0.44, 1 and 1.7 M ratio) compositions. The powders were mechanically alloyed in a planetary ball mill, PM 400 MA type, with stainless steel balls and vials. The balls to powder ratio was 10:1, and the milling occurred for an effective times up to 20 h, at 380 rpm. A solution of ethanol anhydrous was used as process control agent, to prevent heating and sticking to the balls. The as-milled powders were consolidated by spark-plasma sintering (SPS) in a FCT Systeme Gmbh sintering machine, at a pressure of 65 MPa and temperature of 1178 K for a holding time of 5 min.

2.2. Irradiation

The polished surface of one sintered alloy, the CuCrFeTiV equiatomic composition, was irradiated at room temperature with a 300 keV Ar^+ beam to a fluence of 3×10^{20} at/m^2. This fluence was set after the SRIM 2013 [16] program was used to compute the number and distributions of defects caused by the moving argon ions, amounting to an average of ˜100 dpa in the region of deceleration of the ions, prior to stopping [17]. This is the average level of damage expected from neutron irradiation during the foreseeable work cycle of a fusion reactor. The region affected by Ar^+ irradiation is limited to ˜300 nm.

2.3. Materials characterization

After sintering, the geometric density of each sample was measured by the Archimedes method. Metallographic preparation of the samples was performed by grinding with SiC paper and polishing with diamond suspensions (6 μm, 3 μm and 1 μm) and fine polished with colloidal silica suspension (0.2 μm). The microstructures were observed before and after irradiation by secondary electrons (SE) and backscattered electrons (BSE), using a JEOL JSM-7001 F field emission gun scanning electron microscope equipped with an Oxford energy dispersive X-ray spectroscopy (EDS) system. After the irradiation and in order to observe the irradiation damage, samples were observed under a tilt of 50°.

Powder X-ray diffraction measurements of the as-milled samples were performed at room temperature using monochromatic Cu K_α radiation in a Panalytical X´Pert Pro diffractometer with a 2θ–step size of 0.02° from 20° to 80°.

Due to the limited depth of the irradiated region, the X-ray diffraction measurements on the CuCrFeTiV equiatomic sample – were made in a grazing geometry (GIXRD) with an incidence angle of 3° in both conditions, before and after irradiation – employing on a Panalytical X´Pert Pro diffractometer using the Cu $K_{\alpha1}$ and $K_{\alpha2}$ lines, and a Göbel mirror. The ICDD Database [18] was used for phase identification. The Powder Cell software package [19] was used to

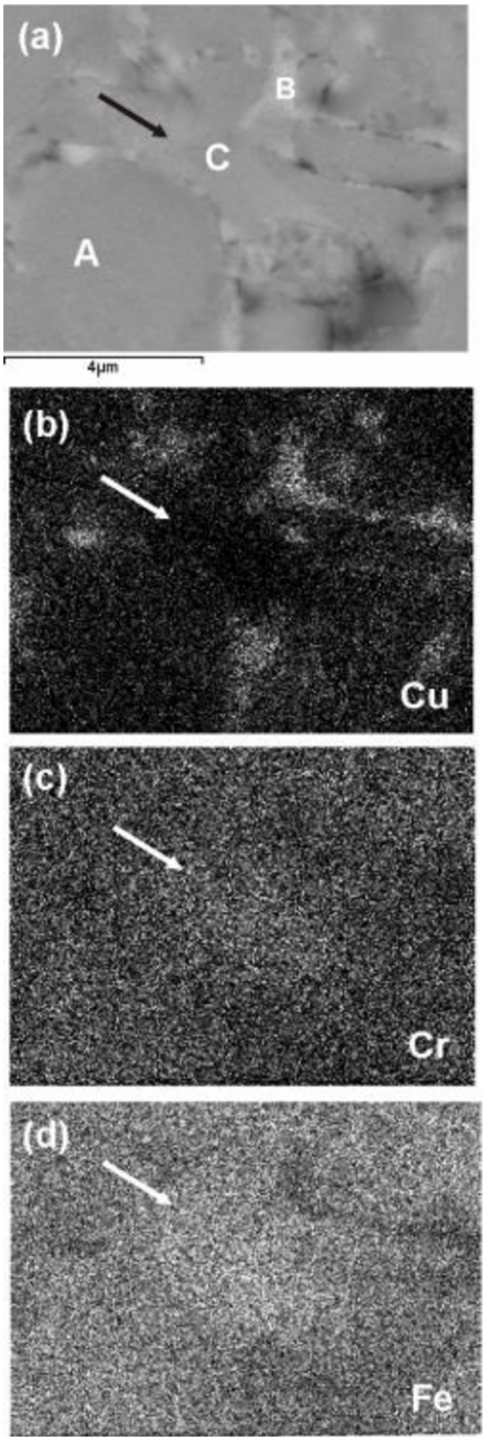

Fig. 2. (a) SE image and corresponding EDS maps for (b) CuKα, (c) Cr-Kα and (d) Fe-Kα radiation from the as-sintered equiatomic CuCrFeTiV sample. The arrow indicates region C.

simulate diffractograms for comparison with experimental data and to refine the lattice parameters. The thermal diffusivity have been investigated using a Netzsch LFA457 Microflash up to 1000 °C.

3. Results and discussion

Fig. 1 displays the microstructure of the as-sintered (a) $Cu_{0.21}CrFeTiV$, (b) $Cu_{0.44}CrFeTiV$, (c) CuCrFeTiV and (d) $Cu_{1.7}CrFeTiV$ samples as seen by SEM. The samples with lower Cu concentrations are very similar and present porosity. The measured densities are also similar in all materials,

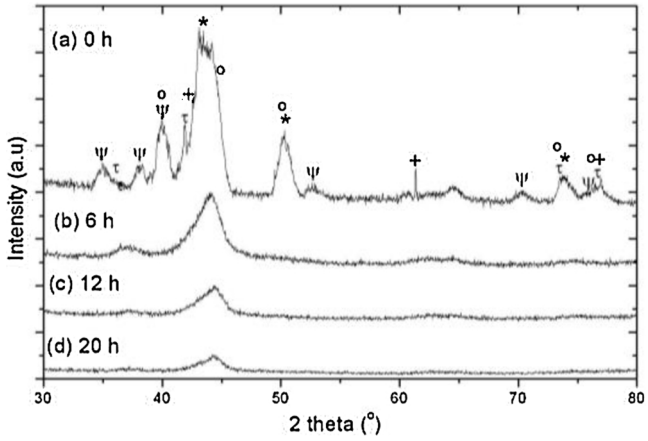

Fig. 3. X-ray diffractogram of as-milled CuCrFeTiV with (a) 0 h, (b) 6 h, (c) 12 h and (d) 20 h. The symbols indicate the correspondent phases: * corresponds to Cu, + corresponds to V, **o** corresponds to Cr_3O, ψ corresponds to $TiO_{0,2}$ and τ corresponds to FeO.

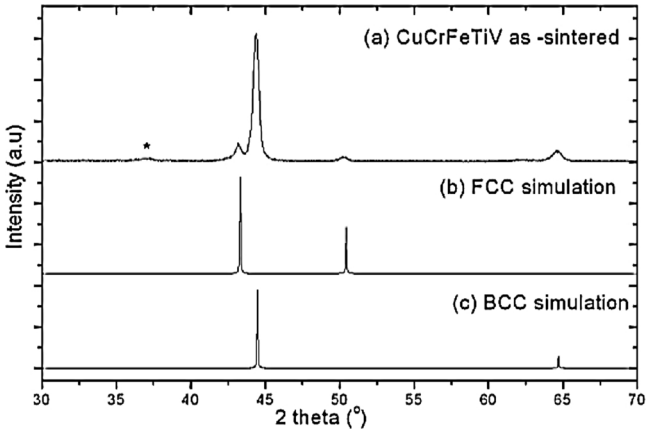

Fig. 4. X-ray diffractogram of (a) as-sintered CrCuFeTiV together with the (b) FCC and (c) BCC crystal structure simulations. The * indicates the presence of TiO.

reaching ˜95%, which indicates ˜5% of porosity. Two different phases, noted as A and B, can be readily identified in Fig. 1. The corresponding EDS elemental maps for the equiatomic CuCrFeTiV composition are shown in Fig. 2. According to the EDS results, region A is chromium rich while region B is copper rich. Moreover, in the EDS elemental maps is possible to observe another phase, indicated as C in Fig. 2. The results evidence a smooth transition between region A and region C, which suggests a relation between both, as a solid solution with increasing atomic concentrations of Cr and Fe and decreasing of Cu. The presence of a copper rich phase (phase B in Fig. 1) can be attributed to the high enthalpy of mixture of copper with the other transition elements (it is only negative, –9 kJ/mol, for the Cu-Ti pair), which indicates a weaker binding force between Cu and the other elements, favouring segregation as opposed to mixing.

Since the microstructure of all samples are similar, only the equiatomic composition CuCrFeTiV was chosen for the X-ray diffraction and irradiation studies. The diffractograms taken from CuCrFeTiV at different stages of milling, between 0 h to 20 h, are presented in Fig. 3. The as-mixed powder (0 h of milling) shows the presence of the pure elements, Cu, V as well as $TiO_{0,2}$, Cr_3O and FeO. Oxidation occured in the mixture since it is possible to identify three oxides $TiO_{0,2,}$ FeO, and the presence of Cr_3O. The results evidence a peak broadening and weakening which increases as the milling time increases (Fig. 3(a) and (e)). Moreover, after 6 h of milling the peaks of elemental powders have disappeared and new phases are formed.

Fig. 4 exhibits the diffractogram of the as-sintered CuCrFeTiV together with simulations of BCC and FCC crystal structure. The

Table 1
Thermodynamic calulations for CuCrFeTiV high entropy alloy.

Composition	ΔH_{mix} (kJ/mol)	δx100	VEC	Δχ
CuCrFeTiV	−2.4	6.15	6.80	0.13

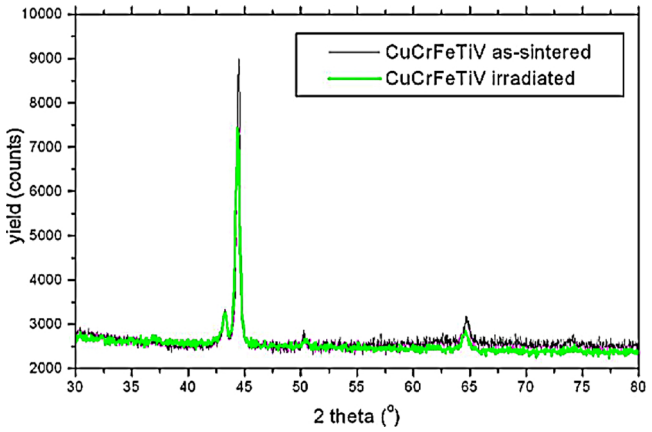

Fig. 5. X-ray diffractogram of the as-sintered and irradiated CrCuFeTiV sample.

diffractogram reveals a major peak of a BCC crystal structure (Fig. 4(c)) assigned with a lattice parameter of 0.2879 nm, and minor peaks of a FCC crystal structure (Fig. 4(b)) although with a lattice parameter of 0.3626 nm. The lattice parameter of the latter FCC structure is very close/nearly equal to the one for pure copper (0.3616 nm [20]).

Based on the microstructural results, the copper rich phase (region B in Fig. 1(c)) should correspond to the FCC crystal structure presented in the diffractogram, since this is a minority phase in the microstructure and the diffractogram evidence minority peaks of this phase. When copper is mixed together with high melting point BCC metals such as chromium and vanadium, it would be expected the formation of a BCC crystal structure upon milling [21], as occurred in this work. However, and probably due to the high content of Cu in CuCrFeTiV, a FCC crystal structure was also found. There are empirical models to predict phase formation in HEAs [22] based on the enthalpies of mixture (ΔH_{mix}) [23], the atomic size differences (δ) [22], the valence electron concentrations (VEC) and the electronegativity differences (Δχ). The calculations of each of those parameters for CuCrFeTiV sample are presented in Table 1. According to S. Guo et. al model [24], solid solutions can be formed with δ(x100) below 6.5 and ΔH_{mix} values between –11.6 and 3.2. Based on the calculations for CuCrFeTiV sample it is expected to have the formation of solid solutions.

Results on thermal diffusivity on these samples between 0 °C and 1000 °C have revealed that the values lay between 0.03 cm^2/s and 0.055 cm^2/s, which are lower than for pure Cu [25] or pure W [26]. Moreover, it was also observed that the values of thermal diffusivity increase with the increasing of Cu content.

The X-ray diffraction results of the as-sintered and irradiated CuCrFeTiV samples are shown in Fig. 5. No significant differences can be observed, which indicates a high stability and resistance of this material to the Ar^+ irradiation. This is also confirmed by the microstructures of CuCrFeTiV high entropy alloy displayed in Fig. 6, where no significant modifications were observed upon irradiation.

In spite of the diferences expected in the nature and distribution of the damage produced by charged ions and neutrons [27], these results are a good indication about the potential of these alloys as thermal barriers in fusion reactors. Further studies, by transmission electron microscopy, to assess the stability of the alloys and the precise nature of the defects as function of the irradiation temperature and fluence are under way.

4. Conclusions

Cu_xCrFeTiV (x = 0.21, 0.44, 1 and 1.7 M ratio) samples produced by mechanical alloying and SPS were studied by SEM, coupled with EDS, and X-ray diffraction. The CuCrFeTiV sample was further irradiated with 300 keV Ar^+ ions to mimic local neutron damage accumulated during a fusion reactor duty cycle.

The results evidence that the samples exhibit very similar multiphasic microstructures. Two phases were observed in the microstructure of the as-sintered materials. The results also show that increasing the Cu content promotes the formation of a larger fraction of a Cu rich phase.

The diffractogram for the as-sintered equiatomic CuCrFeTiV exhibit major peaks of a BCC crystal structure and minor peaks of a FCC crystal structure. Moreover, the last one should correspond the Cu rich region observed in the microstructure. Finally, the work showed that irradiation of CuCrFeTiV does not seem to alter or affect the microstructure and structure, thus implying a high stability and resistance of this CuCrFeTiV high entropy alloy in face of irradiation damage by energetic Ar^+ ions, and, expectedly, to neutron irradiation in fusion reactors as well.

Shall these findings be confirmed as a general trend of such HEA materials, then these will be promising materials to use in future nuclear fusion reactors.

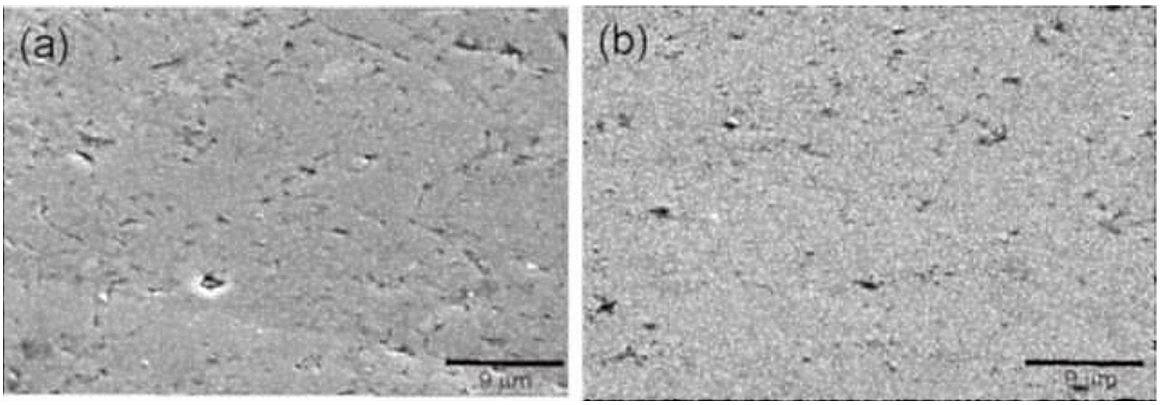

Fig. 6. SEM images with a tilt of 50° evidencing the microstructure of CuCrFeTiV (a) before and (b) after irradiation.

Acknowledgments

This project has received funding from the European Union's Horizon 2020 research and innovation program under grant agreement number 633053. IST activities also received financial support from "Fundação para a Ciência e Tecnologia" through project Pest-OE/SADG/LA0010/2013. The views and opinions expressed herein do not necessarily reflect those of the European Commission. Financial support was also received from the "Fundação para a Ciência e Tecnologia" (FCT) under the PTDC/CTM/100163/2008 grant and the PEST-OE/CTM-UI0084/2011 and UID/Multi/04349/2013 contracts. M. Dias acknowledges the FCT grant SFRH/BPD/68663/2010.

References

[1] N. Baluc, et al., Nucl. Fusion 47 (10) (2007) S696–S717.
[2] K. Sugiyama, et al., Nucl. Fusion 50 (3) (2010) 35001.
[3] V. Barabash, et al., J. Nucl. Mater. 367–370 (A) (2007) 21–32.
[4] X. Zhang, et al., J. Nucl. Mater. 455 (1) (2014) 537–543.
[5] D. Stork, et al., J. Nucl. Mater. 455 (1–3) (2014) 277–291.
[6] A. Li-Puma, et al., Fusion Eng. Des. 88 (9–10) (2013) 1836–1843.
[7] J.W. Yeh, et al., Adv. Eng. Mater. 6 (5) (2004) 299–303.
[8] C.-J. Tong, et al., Metall. Mater. Trans. A 36 (4) (2005) 881–893.
[9] C.-Y. Hsu, et al., Metall. Mater. Trans. A 35 (5) (2004) 1465–1469.
[10] P.-K. Huang, et al., Adv. Eng. Mater. 6 (12) (2004) 74–78.
[11] Y.Y. Chen, et al., Corros. Sci. 47 (9) (2005) 2257–2279.
[12] Y.Y. Chen, et al., Corros. Sci. 47 (11) (2005) 2679–2699.
[13] M.H. Tsai, et al., J. Electrochem. Soc. 158 (11) (2011) H1161.
[14] C.-L. Lu, et al., J. Appl. Crystallogr. 46 (3) (2013) 736–739.
[15] T. Egami, et al., Metall. Mater. Trans. A 45 (1) (2014) 180–183.
[16] Software Package, SRIM, 2013, http://www.srim.org.
[17] M.R. Gilbert, et al., J. Nucl. Mater. 442 (2013) S755–S760.
[18] Http://www.icdd.com, "ICDD PDF-2 DATABASE".
[19] W. Kraus, G. Nolze, Powder Cell for Windows, Version 2.2, Federal Institute for Materials Research and Testing, Berlin, 1999.
[20] http://periodictable.com/Properties/A/LatticeConstants.html.
[21] S. Praveen, et al., J. Miner. Metals Mater. Soc. 65 (12) (2013) 1797–1804.
[22] D.B. Miracle, O.N. Senkov, Acta Mater. 122 (2017) 448–511.
[23] Y. Zhang, Y.J. Zhou, Mater. Sci. Forum 561–565 (2017) 1337–1339.
[24] S. Guo, et al., Intermetallics 41 (2013) 96–103.
[25] E. Breval, J.P. Cheng, D.K. Agrawal, P. Gigl, A. Dennis, R. Roy, A.J. Papworth, Mater. Sci. Eng. A 391 (1 − 2) (2005) 285–295.
[26] M. Futjitsuka, et al., J. Nucl. Mater. 238–287 (2000) 1148–1151.
[27] S.J. Zinkle S, A. Möslang, Fusion Eng. Des. 88 (2013) 472–482.